Journal of Power Sources 244 (2013) 23–28

Contents lists available at SciVerse ScienceDirect

Journal of Power Sources

journal homepage: www.elsevier.com/locate/jpowsour

The effect of thermal stability for high-Ni-content layer-structured cathode materials, $LiNi_{0.8}Mn_{0.1-x}Co_{0.1}Mo_xO_2$ ($x = 0$, 0.02, 0.04)

Hiroaki Konishi*, Masanori Yoshikawa, Tatsumi Hirano

Hitachi Research Laboratory, Hitachi Ltd., 7-1-1 Ohmika-cho, Hitachi, Ibaraki 319-1292, Japan

HIGHLIGHTS

- Thermal stability of $LiNi_{0.8}Mn_{0.1}Co_{0.1}O_2$ was improved by Mo substitution.
- Mo substitution suppressed the crystal structure change from spinel to rock-salt and reduced oxygen release by heating.
- Li-rich Mo-substituted cathode, $Li_{1.10}Ni_{0.8}Mn_{0.06}Co_{0.1}Mo_{0.04}O_2$, satisfied both high capacity and high thermal stability.

ARTICLE INFO

Article history:
Received 8 October 2012
Received in revised form
29 April 2013
Accepted 5 May 2013
Available online 14 May 2013

Keywords:
Lithium ion battery
Cathode
Thermal stability
Oxygen release
Crystal structure change
Mo substitution

ABSTRACT

Improving thermal stability is one of the most serious issues concerning Ni-based cathode materials for Li ion batteries. To increase the capacity for maintaining good thermal stability, we substitute Mo for Mn. We apply differential scanning calorimetry (DSC), thermal desorption spectrometry-mass spectrometry (TDS-MS), and X-ray diffraction (XRD) to elucidate the effect of Mo substitution. The application of DSC indicates that Mo substitution effectively reduces the exothermic reaction between the cathode and electrolyte. The applications of TDS-MS and XRD indicate that Mo substitution suppresses crystal structure change and reduces the oxygen release that accompanies heating below 350 °C. However, the discharge capacities of Mo-substituted samples are lower than that of sample without Mo substitution. We optimize the Li/transition metal ratio and obtain $Li_{1.10}Ni_{0.8}Mn_{0.06}Co_{0.1}Mo_{0.04}O_{2+\delta}$, which satisfy both high capacity and high thermal stability requirements.

1. Introduction

Lithium ion batteries for plug-in hybrid electric vehicles (PHEV) and electric vehicles (EV) are required to be safer and exhibit a higher energy density than conventional batteries. Therefore, high-Ni-content layer-structured cathode materials are expected to be promising as cathode active materials.

It has been reported that increased Ni content increases charge–discharge capacity [1–4]. However, materials with high Ni content are negatively affected by their poor thermal stability, especially at a high charge state [5–8]. It was reported that in $Li_{1-a}NiO_2$ [9–13] and in $Li_{1-a}NiMO_2$ (M: metal) [14–26] the crystal structure of $Li_{1-a}MO_2$ changed from layer to spinel to rock-salt and released oxygen as the temperature increased. In order to improve structural stability, a number of elements, i.e., Co [27–29], Mn [28,30], Ti [28,29,31], Mg [29,32,33], TiMg [34], Al [35–38], Fe [38], Zn [39], Si [40], Ga [41,42], and Mo [43–45], were substituted. In our previous paper [26], we attributed the reason for the instability of Ni-based cathode materials to the instability of the high valence state of Ni. Therefore, the substituted element was selected from the viewpoint of stability in the high valance state. In this research, we focused on substituting Mo for Mn. There are two reasons Mo is thought to be an effective substitute material. First, since its high valence state is more stable than its low valance state, it may be stable at a high charge state. Second, if Mo^{6+} is substituted for Mn^{4+}, the rate of Ni^{2+} to Ni^{3+} increases. Therefore, the Ni valence of Mo-substituted cathode materials is lower than that of non-substituted cathode materials, and this may improve thermal stability. Therefore, we studied the effect of Mo substitution on the thermal stability of Ni-based cathode materials.

We evaluated the exothermic reaction between the cathodes and electrolyte by differential scanning calorimetry (DSC), oxygen release from the cathodes by thermal desorption spectrometry-mass spectrometry (TDS-MS), and crystal structure change by X-ray diffraction (XRD).

* Corresponding author. Tel.: +81 294 52 5111x6089; fax: +81 294 52 7636.
E-mail address: hiroaki.konishi.yj@hitachi.com (H. Konishi).

0378-7753/$ – see front matter © 2013 Elsevier B.V. All rights reserved.
http://dx.doi.org/10.1016/j.jpowsour.2013.05.004

2. Experimental

The cathode materials $LiNi_{0.8}Mn_{0.1-x}Co_{0.1}Mo_xO_2$ (x = 0, 0.02, 0.04) were synthesized by solid state reaction. The stoichiometric amounts of LiOH, NiO, MnO_2, Co_3O_4, and MoO_3 with 3% excess Li were thoroughly mixed and pressed into pellets. The pellets were precalcined in oxygen atmosphere at 600 °C for 10 h. The precalcined materials were then ground and pressed into pellets, which were calcined in oxygen atmosphere at 850 °C for 10 h.

We measured the charge–discharge capacities of these cathode materials. Cathodes were formed on aluminum foil by blade-coating of a slurry consisting of the active material, carbon, polyvinylidene difluoride (PVDF) (85:10:5 wt.%), and *N*-methyl pyrrolidone (NMP) solvent, followed by drying, pressing, and cutting. The delithiated electrodes were prepared according to the following process. Test cells were assembled with a cathode electrode, a lithium metal as an anode electrode, a microporous polypropylene separator, and a 1 M $LiPF_6$ solution of a mixture of carbonate solvents in an argon glove box. The cells were charged and discharged at a C/20 rate between 3.0 and 4.3 V.

Samples for DSC measurement (DSC6100; Seiko Instruments Inc.) were prepared using the following method. Cathodes containing $Li_{1-y}Ni_{0.8}Mn_{0.1-x}Co_{0.1}Mo_xO_2$ (x = 0, 0.02, 0.04) were charged to a prescribed composition (y = 0.8) at a C/20 rate of constant current. After charging, the electrodes were removed from the cells, washed with dimethyl carbonate (DMC), and dried. The charged $Li_{0.2}Ni_{0.8}Mn_{0.1-x}Co_{0.1}Mo_xO_2$ (x = 0, 0.02, 0.04) electrodes were put into a SUS sample pan with 1 ml of electrolyte. They were set in the DSC equipment and heated to 350 °C in argon atmosphere at a rate of 5 °C min^{-1}.

Samples for TDS-MS (EMD-WA-1000; ESCO, Ltd.) were prepared using the same method as that for the DSC samples; the charged $Li_{0.2}Ni_{0.8}Mn_{0.1-x}Co_{0.1}Mo_xO_2$ (x = 0, 0.04) electrodes were set in the TDS-MS sample chamber and heated to 350 °C in a vacuum at a rate of 5 °C min^{-1}. The released oxygen was detected using a quadrupole mass spectrometer with a step of 0.02 s.

Samples for XRD (Rint-2200 UltimaIII; Rigaku) were prepared as follows. The charged $Li_{0.2}Ni_{0.8}Mn_{0.1-x}Co_{0.1}Mo_xO_2$ (x = 0, 0.04) electrodes were heated in argon atmosphere for 1 h at 150–350 °C to expose them to anomalous high temperatures that might occur during unsafe incidents and cooled to room temperature. Then XRD was applied to identify the crystal structures of the prepared samples before and after heating at high temperatures using a Rigaku diffractometer with a graphite monochromator and Cu Kα radiation at 40 kV and 40 mA. The diffraction angles were scanned from 10 to 70° using a step scan method with a step of 0.02° and a counting time of 1.5 s per step.

3. Results and discussion

3.1. Crystal structure of $LiNi_{0.8}Mn_{0.1-x}Co_{0.1}Mo_xO_2$ (x = 0, 0.02, 0.04)

Fig. 1 shows the XRD patterns of $LiNi_{0.8}Mn_{0.1-x}Co_{0.1}Mo_xO_2$ (x = 0, 0.02, 0.04). All the peaks were assigned to a hexagonal α-$NaFeO_2$ structure of the *R*3m space group. Therefore, Mo^{6+} is substituted for Mn^{4+}, and is thought to occupy the octahedral site. Table 1 shows the lattice parameters and intensity ratio of I(003)/I(104). The lattice parameter a increased as Mo content increased. On the other hand, the lattice parameter c changed little regardless of the amount of Mo substitution. The lattice parameter a is related to the change in transition metal ionic size. The ionic sizes of Mo^{6+}(0.59 Å) is closer to that of Ni^{2+}(0.69 Å), Ni^{3+}(0.56 Å), Co^{3+}(0.545 Å), and Mn^{4+}(0.53 Å) than to that of Li^{+}(0.76 Å) [46]. Therefore, Mo^{6+}(0.59 Å) is thought to occupy the transition metal site. As Mo^{6+} is increasingly substituted for Mn^{4+}, the rate of Ni^{2+} to Ni^{3+} increases. Since the ionic sizes of Ni^{2+}(0.69 Å) and Mo^{6+}(0.59 Å) are larger than those of Ni^{3+}(0.56 Å) and Mn^{4+}(0.53 Å) [46], the lattice parameter a increases with increasing Mo substitution. Since the lattice parameter c is related not only to the transition metal ionic size but also to lattice strain and cation mixing, it may not increase monotonically as the Mo content increases. The decreased intensity ratio of I(003)/I(104) indicates that Ni in the Li site increases [47,48]. Mo substitution increases the ratio of Ni^{2+} to Ni^{3+}. Since the ionic size of Ni^{2+}(0.69 Å) is similar to that of Li^{+}(0.76 Å), the degree of cation mixing may be increased.

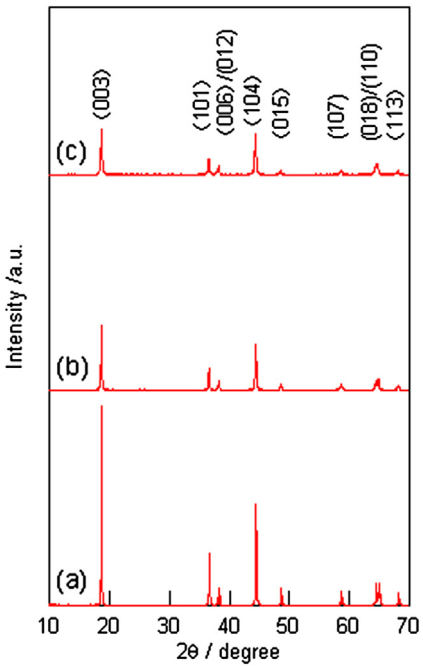

Fig. 1. XRD patterns of $LiNi_{0.8}Mn_{0.1-x}Co_{0.1}Mo_xO_2$ (x = 0, 0.02, 0.04) (a) x = 0, (b) x = 0.02, (c) x = 0.04.

3.2. Charge–discharge capacities of $LiNi_{0.8}Mn_{0.1-x}Co_{0.1}Mo_xO_2$ (x = 0, 0.02, 0.04)

Fig. 2 shows the initial charge–discharge capacities of $LiNi_{0.8}Mn_{0.1-x}Co_{0.1}Mo_xO_2$ (x = 0, 0.02, 0.04) at a C/20 rate between 3.0 and 4.3 V. The discharge capacities of Mo-substituted samples were lower than that of sample without Mo substitution. This leads us to believe that Ni in the Li site disturbs Li diffusion in Mo-substituted samples.

3.3. Exothermic reaction between cathodes and electrolyte by heating

We applied DSC to elucidate the exothermic reaction between the cathodes and electrolyte. Fig. 3 shows the DSC spectra of $Li_{0.2}Ni_{0.8}Mn_{0.1-x}Co_{0.1}Mo_xO_2$ (x = 0, 0.02, 0.04). Heat flow decreased

Table 1
Lattice parameters and intensity ratio of I(003)/I(104) in $LiNi_{0.8}Mn_{0.1-x}Co_{0.1}Mo_xO_2$ (x = 0, 0.02, 0.04).

x	a/Å	c/Å	I(003)/I(104)
0	2.871	14.20	1.95
0.02	2.876	14.22	1.38
0.04	2.882	14.22	1.08

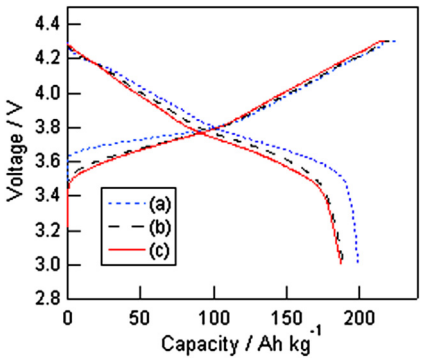

Fig. 2. Initial charge and discharge capacities of $LiNi_{0.8}Mn_{0.1-x}Co_{0.1}Mo_xO_2$ ($x = 0$, 0.02, 0.04) at a C/20 rate between 3.0 and 4.3 V (a) $x = 0$, (b) $x = 0.02$, (c) $x = 0.04$.

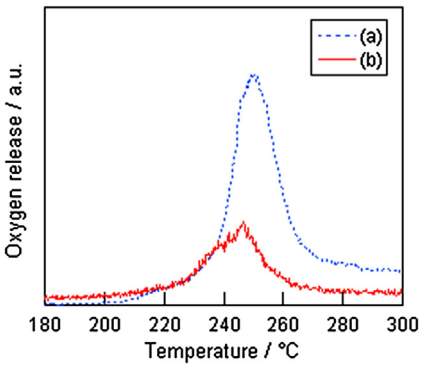

Fig. 4. TDS-MS spectra of $Li_{0.2}Ni_{0.8}Mn_{0.1-x}Co_{0.1}Mo_xO_2$ ($x = 0$, 0.04) (a) $x = 0$, (b) $x = 0.04$.

as the Mo content increased. These results indicate that Mo substitution is effective for improving thermal stability.

3.4. Mechanism for improving thermal stability by Mo substitution

3.4.1. Oxygen release from cathodes incurred by heating

Since DSC was measured in an inert atmosphere, gas released from the cathode is thought to be involved in the exothermic reaction. In applying TDS-MS to elucidate gas release from cathodes, gases such as O_2, HF, and CO_2 were detected. Since the cathode does not contain H or F, we attribute the presence of HF to decomposition of $LiPF_6$ and the electrolyte. Two possibilities can be considered to explain the generation of CO_2. One is that it is generated from the solid state interface (SEI) formed from the reaction between oxygen from the cathode and the electrolyte. The other is that it is generated due to decomposition of the binder and electrolyte. These two causes are indistinguishable, but the sample measured by TDS-MS was a cathode that had been washed by DMC. Therefore, the CO_2 detected by TDS-MS was not related to oxygen from the cathode except for that generated from the SEI formed during the charge reaction. We therefore focused on O_2 because it was released from cathodes by heating and might trigger an exothermic reaction with the electrolyte. Fig. 4 shows TDS-MS spectra of $Li_{0.2}Ni_{0.8}Mn_{0.1-x}Co_{0.1}Mo_xO_2$ ($x = 0$, 0.04). Oxygen release from $Li_{0.2}Ni_{0.8}Mn_{0.06}Co_{0.1}Mo_{0.04}O_2$ was 46% that from $Li_{0.2}Ni_{0.8}Mn_{0.1}Co_{0.1}O_2$ from 25 °C to 350 °C. This indicates Mo substitution is effective in reducing oxygen release from the cathode during heating below 350 °C.

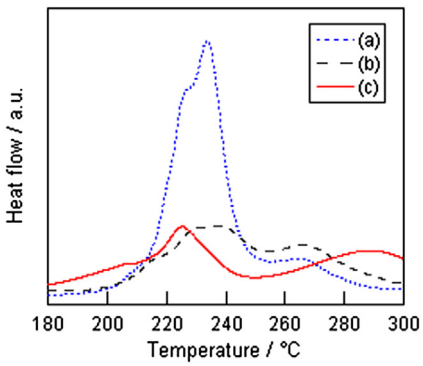

Fig. 3. DSC spectra of $Li_{0.2}Ni_{0.8}Mn_{0.1-x}Co_{0.1}Mo_xO_2$ ($x = 0$, 0.02, 0.04) (a) $x = 0$, (b) $x = 0.02$, (c) $x = 0.04$.

3.4.2. Crystal structure change by heating

It was previously reported that crystal structure change accompanies oxygen release from the cathode by heating [9–26]. Fig. 5 shows the XRD patterns of $Li_{0.2}Ni_{0.8}Mn_{0.1-x}Co_{0.1}Mo_xO_2$ ($x = 0$, 0.04) heated at 150–350 °C. Fig. 5(1) shows the results for $Li_{0.2}Ni_{0.8}Mn_{0.1}Co_{0.1}O_2$. All the peaks were assigned to the layer structure of the *R*3m space group at 150 °C. From 150 to 200 °C, the (018) and (110) peaks at around 65° were merged, and a new diffuse peak at $2\theta = 31°$ emerged, which was characteristic of the spinel structure of the Fd3m space group. This result indicates that the layer structure changes to spinel at 200 °C. Changes also occurred above 250 °C. As the temperature increased, the diffuse peak at $2\theta = 31°$ disappeared. The intensity of the peaks at $2\theta = 19°$, 37° decreased while that of the peak at $2\theta = 38°$ increased. The peaks at $2\theta = 45°$, 65° moved to lower angles. These phenomena correspond to the change to the rock-salt structure of the Fm3m space group. Therefore, the spinel structure gradually changes to rock-salt from 250 °C to 350 °C. Fig. 5(2) shows the results for $Li_{0.2}Ni_{0.8}Mn_{0.06}Co_{0.1}Mo_{0.04}O_2$. The crystal structure change was the same as that for $Li_{0.2}Ni_{0.8}Mn_{0.1}Co_{0.1}O_2$ below 200 °C. However, it was quite different above 250 °C. The peaks at $2\theta = 31°$, 37° did not disappear even at 350 °C. These results indicate that the crystal

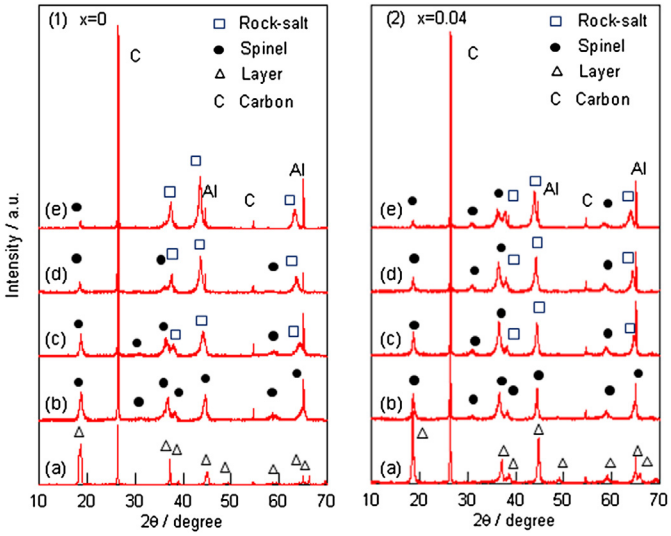

Fig. 5. XRD patterns of $Li_{0.2}Ni_{0.8}Mn_{0.1-x}Co_{0.1}Mo_xO_2$ ($x = 0$, 0.04) heated at (a) 150 °C, (b) 200 °C, (c) 250 °C, (d) 300 °C, (e) 350 °C.

structure change from spinel to rock-salt is suppressed in $Li_{0.2}Ni_{0.8}Mn_{0.06}Co_{0.1}Mo_{0.04}O_2$. It was previously reported that oxygen release from Ni-based cathodes is caused by the following reaction [9,11–13].

$0 < y \leq 0.5$

$$Li_{1-y}MO_2 \rightarrow (1-2y)LiMO_2 + yLiM_2O_4 \quad (1)$$

$y > 0.5$

$$Li_{1-y}MO_2 \rightarrow (2-y)/3[Li_{3(1-y)/(2-y)}M_{(2y-1)/(2-y)}][M]_2O_4 + [(2y-1)/3]O_2 \quad (2)$$

$$(2-y)/3[Li_{3(1-y)/(2-y)}M_{(2y-1)/(2-y)}][M]_2O_4 \rightarrow [Li_{1-y}M]O_{2-y} + [(2-y)/6]O_2 \quad (3)$$

Since the Ni content in $Li_{0.2}Ni_{0.8}Mn_{0.1}Co_{0.1}O_2$ is high, thermal decomposition by heating occurs in accordance with the above formulas. The change from spinel to rock-salt structure is almost completed at 350 °C. If $y = 0.8$ is substituted in Formulas (2) and (3), oxygen release from the cathode will be 0.4, which is 40% of the oxygen contained in $Li_{0.2}MO_2$. For $Li_{0.2}Ni_{0.8}Mn_{0.06}Co_{0.1}Mo_{0.04}O_2$, the crystal structure changes in the same sequence as that without Mo substitution. However, the change from spinel to rock-salt structure is further suppressed even at 350 °C. If $y = 0.8$ is substituted in Formula (2), oxygen release from the cathode will be 0.2, which is half as much as that without Mo substitution. The calculated value is mostly in agreement with the TDS-MS results. This means the effects of Mo are suppressing the crystal structure change from spinel to rock-salt and reducing coincident oxygen release.

3.5. Recovery of reduced capacity by Mo substitution

The $LiNi_{0.8}Mn_{0.06}Co_{0.1}Mo_{0.04}O_2$ cathode proved to be effective for improving thermal stability; however, its discharge capacity was lower than that without Mo substitution, as shown in Fig. 2. Therefore, we tried to recover capacity by optimizing the Li/transition metal (TM) ratio. We prepared $Li_zNi_{0.8}Mn_{0.06}Co_{0.1}Mo_{0.04}O_{2+\delta}$ (z = 1.03, 1.06, 1.09, 1.10, 1.12, 1.18) cathodes. Fig. 6 shows their XRD patterns. No impurities were found except for the z = 1.18 case. Table 2 shows the lattice parameters and intensity ratio of $I(003)/I(104)$. There was little change in lattice parameters a and c except for the z = 1.12, 1.18 case. With increasing Li^+(0.76 Å) content, the valence of Ni partly changes from Ni^{2+}(0.69 Å) to Ni^{3+}(0.56 Å) [46]. It is thought that this is the reason the lattice parameters hardly change. The intensity ratio of $I(003)/I(104)$ for z = 1.06–1.18 was significantly larger than that of z = 1.03; this indicates that excess Li suppresses Ni occupation of the Li site. Excess Li is mainly thought to occupy the Li site. However, since the ionic size of Li^+(0.76 Å) is close to that of Ni^{2+}(0.69 Å), it is possible that Li might occupy the transition metal site in addition to the Li site. It is also possible that excess Li resides in the cathode surface. However, since excess Li is effective in suppressing cation mixing, it is thought that a great portion of excess Li is contained in the crystal.

Fig. 7 shows initial discharge capacities of $Li_zNi_{0.8}Mn_{0.06}Co_{0.1}Mo_{0.04}O_{2+\delta}$ (z = 1.03, 1.06, 1.09, 1.10, 1.12, 1.18). The capacity was dependent on Li/TM, and a Li/TM ratio of 1.10 gave the largest capacity; as much as 197 Ah kg^{-1}, which was almost the same as that of $LiNi_{0.8}Mn_{0.1}Co_{0.1}O_2$ (199 Ah kg^{-1}). This indicates that suppression of Ni in the Li site is effective in increasing discharge capacity.

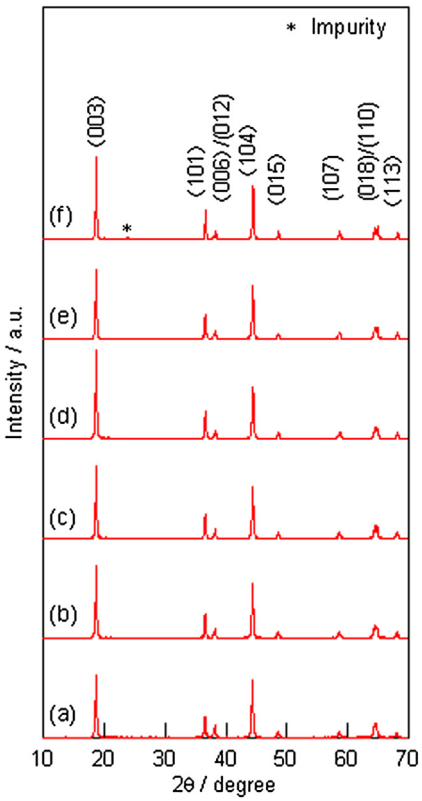

Fig. 6. XRD patterns of $Li_zNi_{0.8}Mn_{0.06}Co_{0.1}Mo_{0.04}O_2$ (a) z = 1.03, (b) z = 1.06, (c) z = 1.09, (d) z = 1.10, (e) z = 1.12 (f) z = 1.18.

3.6. Thermal stability of $Li_{1.10}Ni_{0.8}Mn_{0.06}Co_{0.1}Mo_{0.04}O_{2+\delta}$

Fig. 8 shows the DSC spectra of the heating-produced reaction between the delithiated cathodes and the electrolyte. The $Li_{1.10}Ni_{0.8}Mn_{0.06}Co_{0.1}Mo_{0.04}O_{2+\delta}$ cathode was charged to the same state as the $Li_{0.2}Ni_{0.8}Mn_{0.06}Co_{0.1}Mo_{0.04}O_{2+\delta}$ one to enable comparison with the results for $LiNi_{0.8}Mn_{0.06}Co_{0.1}Mo_{0.04}O_2$ as shown in Fig. 3. It was found that $Li_{1.10}Ni_{0.8}Mn_{0.06}Co_{0.1}Mo_{0.04}O_{2+\delta}$ had thermal stability as good as that of $LiNi_{0.8}Mn_{0.06}Co_{0.1}Mo_{0.04}O_2$. This indicates the Li/TM ratio does not affect the thermal stability of the Mo-substituted samples.

3.7. Discussion

The effects of Mo substitution may be speculated as follows. The layer, $Li_{1-y}MO_2$, and rock-salt, $[Li_{1-y}M]O_{2-y}$, structures have only an octahedral site for occupying metal ions. However, the spinel structure, $[Li_{3(1-y)/(2-y)}M_{(2y-1)/(2-y)}][M]_2O_4$, has both tetrahedral and octahedral sites. When the crystal structure changes from layer to spinel according to Reaction (2), some of the metal ions have to change their site from the octahedral one to the tetrahedral one. The valence of transition metals in $Li_{0.2}MO_2$ is 3.8^+, a valence at

Table 2
Lattice parameters and intensity ratio of $I(003)/I(104)$ in $Li_zNi_{0.8}Mn_{0.06}Co_{0.1}Mo_{0.04}O_{2+\delta}$ (z = 1.03, 1.06, 1.09, 1.10, 1.12, 1.18).

z	a/Å	c/Å	$I(003)/I(104)$
1.03	2.882	14.22	1.08
1.06	2.881	14.22	1.33
1.09	2.881	14.21	1.42
1.10	2.880	14.21	1.69
1.12	2.877	14.21	1.61
1.18	2.873	14.21	1.54

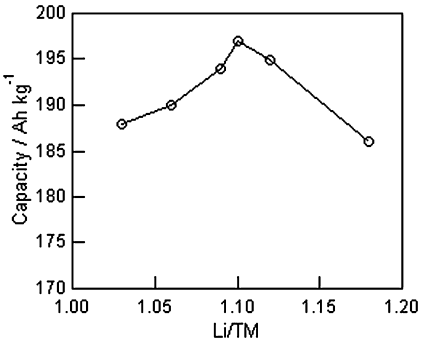

Fig. 7. Initial discharge capacities of $Li_2Ni_{0.8}Mn_{0.06}Co_{0.1}Mo_{0.04}O_{2+\delta}$ ($z = 1.03, 1.06, 1.09, 1.12, 1.18$) at a C/20 rate between 3.0 and 4.3 V.

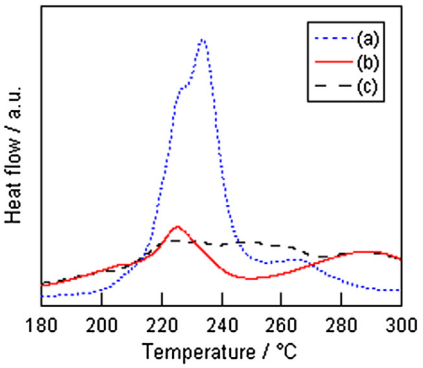

Fig. 8. DSC spectra of cathode materials (a) $LiNi_{0.8}Mn_{0.1}Co_{0.1}O_2$, (b) $LiNi_{0.8}Mn_{0.06}Co_{0.1}Mo_{0.04}O_2$ (c) $Li_{1.1}Ni_{0.8}Mn_{0.06}Co_{0.1}Mo_{0.04}O_{2+\delta}$.

which Ni is unstable. For non-Mo-substituted sample, the Ni ions move from the octahedral site to the tetrahedral one. However, Ni^{3+} and Ni^{4+}, which have 7 and 6 electrons in the d-orbital are more stable in an octahedral site than in a tetrahedral site according to crystal field theory. Therefore, they are likely to move from the tetrahedral site to the octahedral one accompanied by oxygen release at higher temperatures. This may cause the crystal structure to change from spinel to rock-salt with accompanying oxygen release according to Reaction (3).

For Mo-substituted samples, Reaction (3) was suppressed. Since Mo^{6+} has no electrons in the d-orbital, there is no octahedral site stabilization energy according to crystal field theory. Therefore, Mo^{6+} easily moved from the octahedral site to the tetrahedral one when the layer structure was decomposed by heating. However, since Mo^{6+} in the tetrahedral site is stable, the spinel structure is also stable. Consequently, there is no driving force that triggers a crystal structure change from spinel to rock-salt. As a result, Mo is effective in suppressing crystal structure change from spinel to rock-salt rather than from layer to spinel.

4. Conclusion

The cathode material $LiNi_{0.8}Mn_{0.1}Co_{0.1}O_2$ has high capacity but its thermal stability is not good; we mitigated this defect by Mo substitution. The discharge capacities of Mo-substituted samples were lower than that of non-substituted sample. However, Mo was found to be effective in improving thermal stability. Applying DSC showed that exothermic reaction between the cathode and electrolyte was suppressed by Mo substitution. Applying XRD and TDS-MS indicated that Mo substitution was effective in suppressing crystal structure change from spinel to rock-salt and oxygen release caused by the change due to heating. In attempting to recover capacity by optimizing the Li/transition metal ratio, we obtained $Li_{1.10}Ni_{0.8}Mn_{0.06}Co_{0.1}Mo_{0.04}O_{2+\delta}$, which satisfied both high capacity and high thermal stability requirements.

Acknowledgments

This work was supported by New Energy and Industrial Technology Development Organization (NEDO) of Japan as a part of the Li-EAD Project. The authors would like to express their thanks to those who participated in the projects. They also thank Prof. T. Horiba of Mie University for his encouraging and helpful discussions concerning this paper.

References

[1] J.R. Dahn, U. von Sacken, M.W. Juzkow, H. Al-Janaby, J. Electrochem. Soc. 138 (1991) 2207–2211.
[2] T. Ohzuku, A. Ueda, M. Nagayama, J. Electrochem. Soc. 148 (1993) 1862–1870.
[3] K.-S. Lee, S.-T. Myung, K. Amine, H. Yashiro, Y.-K. Sun, J. Electrochem. Soc. 154 (2007) A971–A977.
[4] A. Deb, U. Bergmann, S.P. Cramer, E.J. Cairns, J. Electrochem. Soc. 154 (2007) A534–A541.
[5] J.R. Dahn, E.W. Fuller, M. Obrovac, U. Von Sacken, Solid State Ionics 69 (1994) 265–270.
[6] D.D. MacNeil, Z. Lu, Z. Chen, J.R. Dahn, J. Power Sources 108 (2002) 8–14.
[7] H. Arai, M. Tsuda, K. Saito, M. Hayashi, Y. Sakurai, J. Electrochem. Soc. 149 (2002) A401–A406.
[8] S. Jouanneau, D.D. MacNeil, Z. Lu, S.D. Beattie, G. Murphy, J.R. Dahn, J. Electrochem. Soc. 150 (2003) A1299–A1304.
[9] H. Arai, S. Okada, Y. Sakurai, J. Yamaki, Solid State Ionics 109 (1998) 295–302.
[10] H. Arai, Y. Sakurai, J. Power Sources 81–82 (1999) 401–405.
[11] M. Guilmard, L. Croguennec, D. Denux, C. Delmas, Chem. Mater. 15 (2003) 4476–4483.
[12] K.-K. Lee, W.-S. Yoon, K.-B. Kim, K.-Y. Lee, S.-T. Hong, J. Power Sources 97–98 (2001) 321–325.
[13] K.-K. Lee, W.-S. Yoon, K.-B. Kim, K.-Y. Lee, S.-T. Hong, J. Electrochem. Soc. 148 (2001) A716–A722.
[14] K.-K. Lee, W.-S. Yoon, K.-B. Kim, J. Electrochem. Soc. 148 (2001) A1164–A1170.
[15] W.-S. Yoon, M. Balasubramanian, X.-Q. Yang, J. McBreen, J. Hanson, Electrochem. Solid State Lett. 8 (2005) A83–A86.
[16] W.-S. Yoon, K.Y. Chung, M. Balasubramanian, J. Hanson, J. McBreen, X.-Q. Yang, J. Power Sources 163 (2006) 219–222.
[17] W.-S. Yoon, J. Hanson, J. McBreen, X.-Q. Yang, Electrochem. Commun. 8 (2006) 859–862.
[18] K.-W. Nam, W.-S. Yoon, X.-Q. Yang, J. Power Sources 189 (2009) 515–518.
[19] M. Guilmard, L. Croguennec, C. Delmas, Chem. Mater. 15 (2003) 4484–4493.
[20] H. Bang, D.-H. Kim, Y.C. Bae, J. Prakash, Y.-K. Sun, J. Electrochem. Soc. 155 (2008) A952–A958.
[21] S.-T. Myung, A. Ogata, K.-S. Lee, S. Komaba, Y.-K. Sun, H. Yashiro, J. Electrochem. Soc. 155 (2008) A374–A383.
[22] I. Belharouak, D. Vissers, K. Amine, J. Electrochem. Soc. 153 (2006) A2030–A2035.
[23] I. Belharouak, W. Lu, D. Vissers, K. Amine, Electrochem. Commun. 8 (2006) 329–335.
[24] I. Belharouak, W. Lu, J. Liu, D. Vissers, K. Amine, J. Power Sources 174 (2007) 905–909.
[25] N. Yabuuchi, Y.-T. Kim, H.H. Li, Y. Shao-Horn, Chem. Mater. 20 (2008) 4936–4951.
[26] H. Konishi, T. Yuasa, M. Yoshikawa, J. Power Sources 196 (2011) 6884–6888.
[27] J. Cho, H. Jung, Y. Park, G. Kim, H.S. Lim, J. Electrochem. Soc. 147 (2000) 15–20.
[28] H. Arai, S. Okada, Y. Sakurai, J. Yamaki, J. Electrochem. Soc. 144 (1997) 3117–3125.
[29] B.V.R. Chowdari, G.V. Subba Rao, S.Y. Chow, Solid State Ionics 140 (2001) 55–62.
[30] M.-H. Kim, H.-S. Shin, D. Shin, Y.-K. Sun, J. Power Sources 159 (2006) 1328–1333.
[31] H. Liu, J. Li, Z. Zhang, Z. Gong, Y. Yang, Electrochim. Acta 49 (2004) 1151–1159.
[32] J. Cho, Chem. Mater. 12 (2000) 3089–3094.
[33] J. Xiang, C. Chang, F. Zhang, J. Sun, J. Electrochem. Soc. 155 (2008) A520–A525.
[34] Y. Gao, M.V. Yakovleva, W.B. Ebner, Electrochem. Solid State Lett. 1 (1998) 117–119.
[35] T. Ohzuku, A. Ueda, M. Kouguchi, J. Electrochem. Soc. 142 (1995) 4033–4039.
[36] M. Guilmard, C. Pouillerie, L. Croguennec, C. Delmas, Solid State Ionics 160 (2003) 39–50.
[37] S.B. Majumder, S. Nieto, R.S. Katiyar, J. Power Sources 154 (2006) 262–267.
[38] K.K. Lee, W.S. Yoon, K.B. Kim, K.Y. Lee, S.T. Hong, J. Power Sources 97–98 (2001) 308–312.
[39] G.T.K. Fey, J.G. Chen, V. Subramanian, T. Osaka, J. Power Sources 112 (2002) 384–394.
[40] S.-H. Na, H.-S. Kim, S.-I. Moon, Solid State Ionics 176 (2005) 313–317.

[41] M. Balasubramanian, J. McBreen, K. Pandya, K. Amine, J. Electrochem. Soc. 149 (2002) A1246–A1249.
[42] C.J. Han, W.S. Eom, S.M. Lee, W.I. Cho, H. Jang, J. Power Sources 144 (2005) 214–219.
[43] S.-H. Park, S.W. Oh, Y.-K. Sun, J. Power Sources 146 (2005) 622–625.
[44] L.Q. Wang, L.F. Jiao, H. Yuan, J. Guo, M. Zhao, H.X. Li, Y.M. Wang, J. Power Sources 162 (2006) 1367–1372.
[45] S. Sivaprakash, S.B. Majumder, S. Nieto, R.S. Katiyar, J. Power Sources 170 (2007) 433–440.
[46] R.D. Shannon, Acta Crystallogr. A 32 (1976) 751–767.
[47] W. Li, J.N. Reimers, J.R. Dahn, Phys. Rev. B 46 (1992) 3236–3246.
[48] C. Delmas, M. Menetrier, L. Croguennec, I. Saadoune, A. Rougier, C. Pouillerie, G. Prado, M. Grune, L. Fournes, Electrochim. Acta 45 (1999) 243–253.